— 4 —

Source Standards for the Radiometric Calibration of Astronomical Instruments in the VUV Spectral Range Traceable to the Primary Standard BESSY

JÖRG HOLLANDT
Physikalisch-Technische Bundesanstalt
Berlin, Germany

MICHAEL KÜHNE
Physikalisch-Technische Bundesanstalt
Berlin, Germany

MARTIN C.E. HUBER
International Space Science Institute
Bern, Switzerland

BURKHARD WENDE
Physikalisch-Technische Bundesanstalt
Berlin, Germany

On the basis of a high-current hollow-cathode discharge we have developed two transfer source standards suitable for the radiometric calibration of vacuum-ultraviolet (VUV) telescopes. The source standards are transportable and (in their current design) produce collimated beams of 5 mm (grazing-incidence region) and 2.5 mm, 5 mm, 10 mm and 15 mm (normal-incidence region) diameter. By irradiating the entrance aperture of the telescope with this beam, the overall spectral response of the instrument can be determined and spectral-responsivity variations over the entrance aperture can be directly evaluated. The transfer standards described in this paper have been calibrated in the radiometry laboratory of the Physikalisch-Technische Bundesanstalt (PTB) by use of the calculable spectral photon flux of the Berlin electron storage ring for synchrotron radiation BESSY I: a primary radiometric VUV source standard. The output of the source standards has been determined at 57 emission lines covering the wavelength range 15 nm to 150 nm. The photon flux in these emission lines ranges from 10^4 s^{-1} to 10^9 s^{-1} and the overall relative standard uncertainty of the photon flux in any given line is found to be not more than 8 %.

Note: This paper is an updated version of J. Hollandt et al., 1996, *A&AS* **115**, 561

4.1 Introduction

The radiometric calibration of instruments is based on either source or detector standards. Since in the vacuum-ultraviolet (VUV) spectral domain reliable celestial standards are still being established, the radiometric calibration of space-borne VUV instruments must be based on laboratory standards.

In the past, calibrations in the vacuum-ultraviolet have been made almost exclusively by use of detector standards rather than source standards. The detector standard was used to determine the photon flux entering the telescope when the complete instrument was illuminated with a monochromatic photon beam. The ratio of the instrument detector response

and the measured monochromatic flux entering the telescope then represented the spectral responsivity of the complete instrument at this particular wavelength. This procedure was repeated at different wavelengths in order to establish the wavelength-dependent spectral responsivity of the instrument. For practical reasons, in many cases the overall calibration was made in two (or more) steps: the transmission of the telescope and the responsivity of the spectrometer-detector system had to be measured separately [*Reeves et al.*, 1977].

A wide variety of VUV detector standards is available in the form of photoemission diodes [*Canfield and Swanson*, 1987], sodium-salicilate-based detectors [*Philips*, 1984], proportional counters [*Henke and Tester*, 1975; *Kroth et al.*, 1990] or photoelectric ionization chambers [*Samson*, 1964; *Samson and Haddad*, 1974]. The relative uncertainties of these detector standards are of the order of 10 % (1σ), and, particularly for photoemission diodes and sodium-salicilate-based detectors, long-term stability is a problem. The possibilities offered by the significantly lower uncertainties that have been achieved using electrical substitution radiometers operating at liquid-helium temperature as the primary detector standard [*Rabus et al.*, 1997; *Shaw et al.*, 1999] will be briefly addressed in Section 4.5 of this paper.

In contrast to the rather complex procedures that are required to accommodate the use of detector standards, a radiometric instrument calibration based on source standards is straightforward. If the radiation of the source is well-matched to the demands of the calibration and a level of uncertainty of a few percent is sufficient, the instrument to be calibrated is illuminated with the source of known spectral emission and the spectral response of the detector is measured. This classical approach to radiometric calibration could not, however, be used in the VUV until about two decades ago, since such sources were not available.

During the last two decades, VUV source standards – in particular, dedicated electron storage rings (in fact, the primary radiometric VUV standard) – have become available and several instruments have been calibrated with the SURF-II storage ring at the U.S. National Institute of Standards and Technology (NIST) [*Furst et al.*, 1995]. Similar activities took place at the positron storage ring SUPER-ACO at the Institut d'Astronomie Spatiale (IAS) at Orsay [*Besson et al.*, 1989].

The spectral distribution of radiation at most synchrotron sources (see Figure 4.1 for BESSY I) is usually not well matched to the VUV emission of the Sun or other stars. The increase of photon flux with decreasing wavelength of the typical synchrotron source can cause extremely high contributions from high orders of the spectrometer grating, especially for grazing-incidence optics. In order to overcome some of the major difficulties that occur when space instruments are calibrated by direct use of synchrotron radiation, we have developed transfer source standards. Being based on a conventional emission-line source (a hollow-cathode discharge source) with a collimated output beam, our transfer standards avoid the problems associated with the uncollimated, spectrally-continuous, synchrotron radiation, whose polarization, moreover, varies with the viewing angle. The hollow-cathode discharge source we describe here emits well-separated emission lines and thus avoids the often severe problem of high-order contributions that occur in grating instruments. It also provides a wavelength calibration as a matter of course. The transfer standards in question are transportable and can, accordingly, be mounted on the test tank in the laboratory, where the instrument to be calibrated has been developed. Thus there is no need for a special calibration tank nor is there a need to transport the instrument for calibration. This also removes schedule incompatibilities as they are bound to occur with the

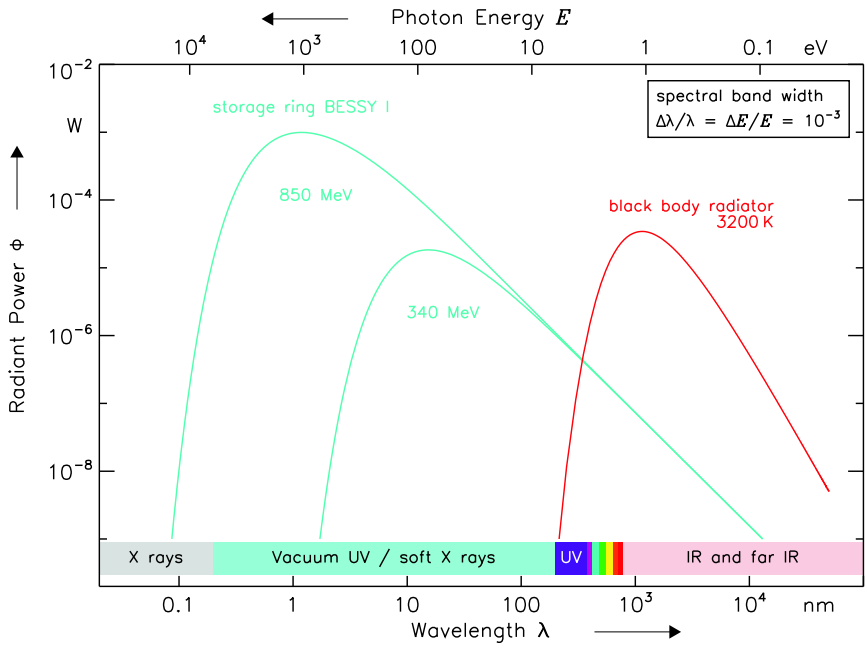

Figure 4.1: Comparison of a black-body radiator at a temperature of 3200 K and the synchrotron-radiation spectrum of the electron storage ring BESSY I at an electron energy of 340 MeV and 850 MeV.

inflexible beam-scheduling that is mandatory for multi-purpose storage ring facilities. A given transfer standard can, in principle, also be brought to different instruments so that an intercalibration by use of the same standard can be achieved. A further interesting property of our transfer source standards is that they produce detector count-rates in the telescope systems under calibration which are comparable with those expected for the instruments when in flight.

4.2 Transfer Source Standards

4.2.1 Hollow-cathode Source

The source standards for the measurement of the spectral responsivity of astronomical instruments are based on a high-current, hollow-cathode, glow-discharge source (Figure 4.2). This source emits intense, unpolarized, line-radiation from the buffer gas and the cathode material (99.5 % aluminium) at wavelengths above 15 nm (Figure 4.3). Equipped with a compact, two-stage, differential pumping system, the source allows windowless observation of its VUV radiation under ultrahigh-vacuum conditions. The flux-limiting aperture stop with a diameter of 0.6 mm is part of the differential pumping system.

As a radiometric transfer standard the source is operated with a fixed current (e.g., 1 A) with a current stability better than 1 mA. The voltage drop over the hollow-cathode discharge (e.g., 500 V) is sensitive to buffer-gas pressure (typically 1 mbar). It can be sta-

bilized (to better than ± 1 V) by regulating the buffer-gas flow with an automatic needle-valve (Balzers RME 010) and a self-regulating voltage control unit. In this mode of operation, the radiant intensity of the VUV emission lines is reproducible within ± 5 % over a period of 40 operating hours.

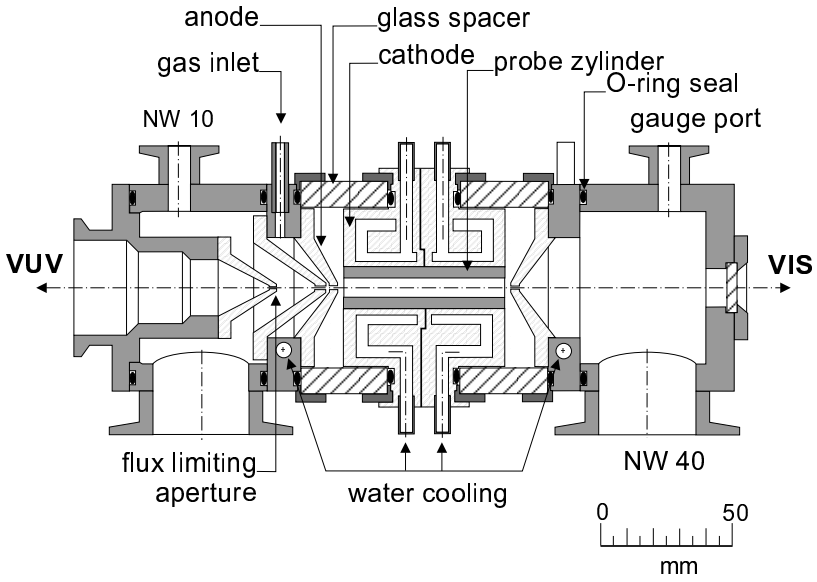

Figure 4.2: Longitudinal section of the hollow-cathode source with an integrated two-stage, differential pumping system.

In order to provide a large number of calibration lines within the spectral range from 15 nm to 150 nm, the hollow-cathode source is alternately operated with various rare gases serving as the buffer gas. Changing the buffer gas does not affect the reproducibility of the emission values, if measures are taken to fully drive out the preceding buffer gas from the discharge tube. After 40 hours of operation the source has to be cleaned of sputtered cathode material and the aluminium cathode cylinder has to be replaced. To reproduce the old photon-flux after cleaning the source, the oxide layer from the fresh aluminium cathode has to be removed, otherwise this layer severely limits the sputtering coefficient of aluminium atoms from the cathode. This can be accomplished by discharge-cleaning when the source is operated with argon for one to two hours with a current of at least 1 A. Over a period of three years the hollow-cathode discharge has been operated for more than 1000 hours without any detectable systematic changes in its radiant intensity. Detailed descriptions of its operation and radiometric characterization as a standard of radiant intensity are given in *Danzmann et al.* [1988] and *Hollandt et al.* [1994].

4.2.2 Source Standards

To serve as a transfer standard for the radiometric calibration of astronomical instruments, the hollow-cathode source has to be combined with adequate optics to convert the diverging radiation of the source into a collimated beam. To cover the spectral range from

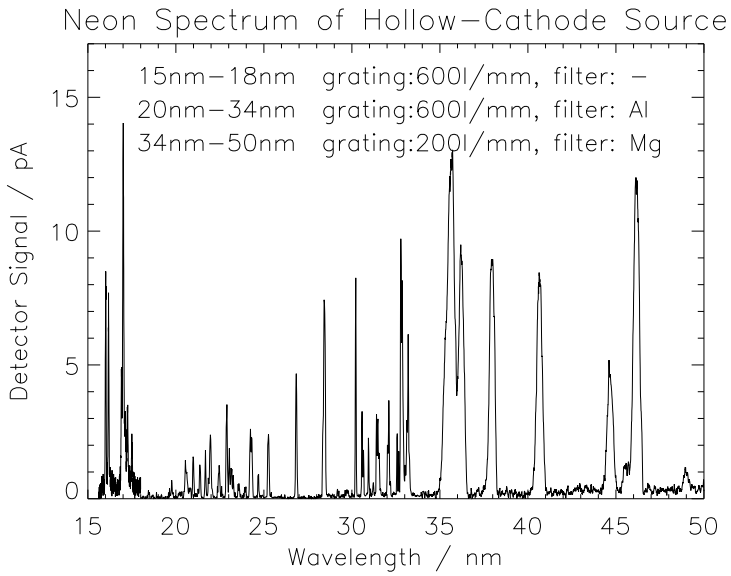

Figure 4.3: Spectrum of the hollow-cathode discharge, showing line emission from multiply-ionized aluminium and neon ions. The spectrum was measured with three different configurations of the toric-grating monochromator beam line.

15 nm to 150 nm with suitable, collimated, spectral photon flux, two telescope-calibration standards, one working in grazing incidence the other in normal incidence, have been developed [*Hollandt et al.*, 1993].

Grazing-incidence Source Standard:
In the grazing-incidence spectral range, a Wolter type-II telescope with an effective focal length of 2.120 m is used to provide a collimated beam (Figure 4.4). The aperture stop of the hollow-cathode source is placed at the focus of the Wolter telescope. The diameter of the collimated beam is limited to 5 mm when it leaves the telescope. The complete transfer standard is mounted on a platform that can be moved up and down ($\pm$150 mm) to allow a precise vertical mapping of the primary telescope mirror of the instrument for calibration with the collimated radiation.

Normal-incidence Source Standard:
To provide collimated VUV radiation above 50 nm, the flux-limiting aperture stop of the hollow-cathode source is placed at the focus of a gold-coated, concave mirror with a focal length of 1.090 m (Figure 4.5). The angle of incidence between the mirror normal and the incoming radiation is 3°. The diameter of the collimated radiation is limited to 10 mm (standard diameter) on the mirror surface. (Since the limiting aperture is mounted on a precisely moveable linear feedthrough, apertures resulting in diameters of the beam of 2.5 mm, 5 mm, and 15 mm are also available.) The spherical collimating mirror can be tilted about two perpendicular axes ($\pm$20 mrad). In the case that the instrument to be calibrated also posseses the ability to tilt its primary mirror this allows a two-dimensional mapping of the primary telescope mirror with the collimated radiation.

Table 4.1: Radiant power of the grazing-incidence source standard in the He I resonance line at 58.43 nm over a period of thirteen months.

Emission line	Radiant Power April '92	Radiant Power August '92	Radiant Power November '92	Radiant Power May '93
58.43 nm He I	605 pW	608 pW	591 pW	630 pW

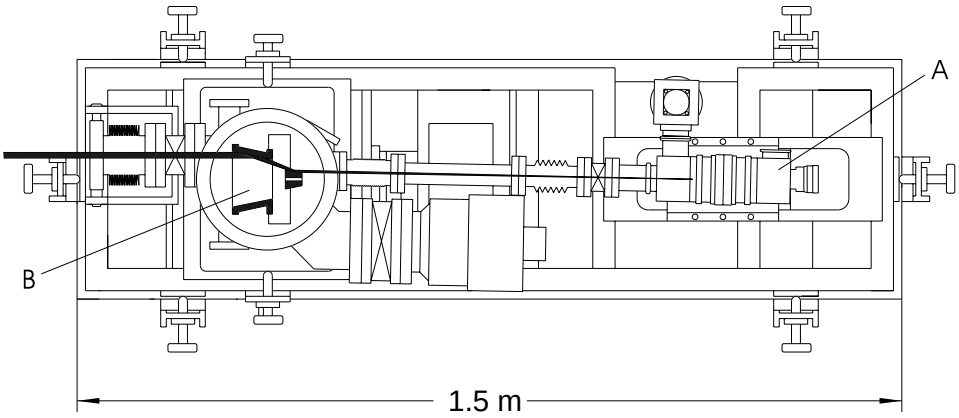

Figure 4.4: Schematic drawing of the grazing-incidence source standard. The diverging radiation from the hollow-cathode source (A) is collimated by a Wolter type-II telescope (B).

The hollow-cathode discharge of the grazing-incidence source standard is operated at a fixed working point of 2 A and 400 V. Since the emission lines of highly-ionized ions typically show a pronounced superlinear current dependence of their radiant intensity, the 2-A/400-V working point provides sufficient photon flux in the 15 nm to 50 nm spectral range, where the spectrum of the source is dominated by doubly- and triply-ionized neon and aluminium emission lines. For the normal-incidence source standard a working point of 1 A and 500 V has been chosen. Under these conditions, the neutral and singly-ionized buffer-gas emission lines that predominate in the spectrum of the source above 50 nm appear with adequate flux.

As an example of the radiometric, long-term stability of the hollow-cathode source the radiant power of the grazing-incidence source standard in the He I resonance line at 58.43 nm is given in Table 4.1 for a period of thirteen months. During this period, the aluminium cathode was replaced 22 times and the source was transported three times between the storage ring BESSY in Berlin and the Rutherford Appleton Laboratory near Oxford, UK, to enable the ground-based calibration of CDS (Coronal Diagnostic Spectrometer).

The vacuum systems of both source standards are made of stainless steel and built according to ultrahigh-vacuum standards. Hollow-cathode sources and mirror chambers are pumped by turbomolecular pumps. Typical pressures in the mirror chambers are in the lower 10^{-8} mbar range when the hollow-cathode source is not in operation. Pressures in the mirror chambers go up into the 10^{-6} mbar range when the discharge is operated with rare gases.

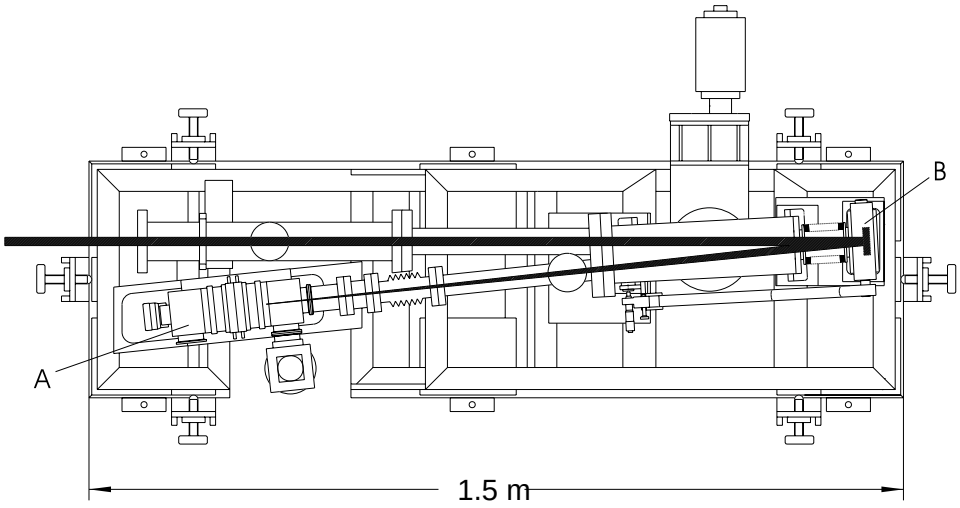

Figure 4.5: Schematic drawing of the normal-incidence source standard. The diverging radiation from the hollow-cathode source (A) is collimated by a concave, gold-coated mirror (B).

4.3 Calibration Procedure of the Transfer Source Standards

In order to perform the spectral-responsivity calibration of astronomical instrumentation, the photon flux in the emission lines of the collimated radiation of the transfer source standards must be known. The spectral radiant flux for a given collection geometry of synchrotron radiation from an electron storage ring is calculable according to Schwinger's formula [*Schwinger*, 1949] from three storage ring parameters: electron energy, magnetic field in the bending magnet, and the current represented by the electrons in the ring. Thus, well-characterized electron storage rings are primary radiometric source standards for radiation which extends from the far-infrared to the X-ray region. PTB had set up a radiometric laboratory at the Berlin electron storage ring BESSY I, which was a storage ring dedicated, among other things, to VUV radiometry. In this laboratory, special beam-lines have been developed for the radiometric characterization of VUV sources. (Note: BESSY I closed down in November 1999 and the radiometry laboratory of PTB was transfered to BESSY II. All the work described in this paper has been performed at BESSY I.) The radiometric calibration is performed on these beam lines by comparing the unknown radiation of transfer standards with the calculable synchrotron radiation of the primary standard BESSY I. The photon flux in the emission line of a transfer standard Φ^{TS} is determined by comparing the detected photocurrent $i^{TS}(\lambda)$ of the transfer standard with the detected photocurrent $i^{SR}(\lambda)$ of the calculable spectral photon flux of the synchrotron radiation $\Phi_\lambda^{SR}(\lambda)$ (for details see *Fischer et al.* [1986] and *Hollandt et al.* [1992]):

$$\Phi^{TS} = \int \Phi_\lambda^{TS}(\lambda)\,\mathrm{d}\lambda = \int \left[i_0^{TS}(\lambda) / i_0^{SR}(\lambda) \right] \Phi_\lambda^{SR}(\lambda) F_0(\lambda)\,\mathrm{d}\lambda \tag{4.1}$$

$$\Phi^{TS} = \int \Phi_\lambda^{TS}(\lambda)\,\mathrm{d}\lambda = \int \left[i_{90}^{TS}(\lambda)/i_{90}^{SR}(\lambda) \right] \Phi_\lambda^{SR}(\lambda) F_{90}(\lambda)\,\mathrm{d}\lambda \tag{4.2}$$

The subscripts 0 and 90 indicate the orientation of the optical plane of the instrumentation used for the flux comparison with respect to the electron orbit plane. The term $F(\lambda)$ describes the different degrees of polarization of the two sources and the polarizing property of the instrumentation used for the flux comparison.

4.3.1 Grazing-incidence Monochromator Beam Line

In the 15 nm to 60 nm spectral range the calibration has been performed with a grazing-incidence, toric-grating, monochromator (TGM) beam line [*Fischer et al.*, 1986]. For the radiometric comparison, an ellipsoidal focusing-mirror can image either the tangent point of the storage ring or the aperture stop of the hollow-cathode source into the entrance slit of the monochromator in such a way that, for both sources, the image of the source is not limited in width or height by the size of the entrance slit (Figure 4.6). The monochromator is moved along its optical axis to compensate for the different image distances of the two sources. Measurements have been performed with a grating of 600 lines/mm (15 nm to 32 nm) and of 200 lines/mm (22 nm to 60 nm). To allow for corrections caused by the different degrees of polarization of the transfer standard and the synchrotron radiation, the monochromator can be rotated by 90 ° around its optical axis, which is defined by the center of the entrance slit and the center of the grating. This allows measurements with the optical plane of the instrument parallel and perpendicular to the plane of the electron orbit. The polarizing property of the monochromator-detector system $M^{MD}(\lambda)$ is determined from measurements of the completely polarized synchrotron radiation in both orientations of the monochromator,

$$M^{MD}(\lambda) = \frac{1 + P^{SR}(\lambda)\, M^{E}(\lambda)}{P^{SR}(\lambda) + M^{E}(\lambda)} \cdot \frac{i_0^{SR}(\lambda) - i_{90}^{SR}(\lambda)}{i_0^{SR}(\lambda) + i_{90}^{SR}(\lambda)} \tag{4.3}$$

The polarizing property of the ellipsoidal focusing mirror $M^{E}(\lambda)$ is calculated by use of the Fresnel formulae. The degree of linear polarization is defined as

$$P(\lambda) = \frac{\Phi_\lambda^{\parallel}(\lambda) - \Phi_\lambda^{\perp}(\lambda)}{\Phi_\lambda^{\parallel}(\lambda) + \Phi_\lambda^{\perp}(\lambda)} \tag{4.4}$$

$\Phi_\lambda^{\parallel}(\lambda)$ and $\Phi_\lambda^{\perp}(\lambda)$ are the components of the spectral radiant power with the electric-field vector oscillating parallel and perpendicular to the plane of the electron orbit. With equations 4.3 and 4.4 the wavelength-dependent functions $F_0(\lambda)$ and $F_{90}(\lambda)$ in equations 4.1 and 4.2 are given by

$$F_{0/90}(\lambda) = \frac{1 \pm P^{SR} M^{MD} + M^{E} \cdot (P^{SR} + M^{MD})}{1 \pm P^{TS} M^{MD} + M^{E} \cdot (P^{TS} + M^{MD})} \tag{4.5}$$

For the radiometric calibration, knowledge of the percentage of radiation diffracted into the higher orders of the synchrotron radiation spectrum is essential. Therefore, the high-order performance of the gratings has been measured [*Kühne and Müller*, 1989]. Additionally, in specific wavelength ranges, absorption-edge filters (Al: 20 nm – 32 nm,

Mg: 25 nm – 41 nm, Sn: 53 nm – 59 nm) have been used behind the exit slit to suppress the influence of synchrotron radiation diffracted in higher order, and the storage ring has been operated with a reduced electron-beam energy of 340 MeV (vs. the standard energy of 800 MeV), which reduced the photon flux on the short-wavelength side of the synchrotron radiation spectrum significantly.

4.3.2 Normal-incidence Monochromator Beam Line

Complementary to the grazing-incidence beam line, a normal-incidence monochromator (NIM) beam line has been used for the calibration of selected emission lines above 40 nm (Figure 4.7). This beam line consisted of an aperture stop (defining the solid angle of the accepted synchrotron radiation), a spherical imaging mirror, a 15 ° McPherson-type monochromator and a photomultiplier detector. Again, the instrumentation is built for the comparison of a transfer standard with the primary standard BESSY. For that purpose, the entire instrumentation can be rotated around a vertical axis, which permits the spherical mirror to form alternately an image of the tangent point of the storage ring or the aperture stop of the hollow-cathode source in the entrance slit of the monochromator. As in the case of the toric-grating monochromator, the size of the entrance slit does not limit the radiant flux of either source. The different distances of the two sources under comparison require that the normal-incidence monochromator can be moved along its optical axis. In contrast to the TGM beam line, the complete normal-incidence instrumentation (including the imaging mirror) can be rotated by 90 ° about its horizontal axis, which coincides with the optical entrance axis. By measuring the synchrotron radiation with the optical plane of the instrumentation both parallel and perpendicular to the plane of the electron orbit, the polarizing property of the mirror-monochromator-detector system $M(\lambda)$ is determined by

$$M(\lambda) = \frac{1}{P^{SR}(\lambda)} \cdot \frac{i_0^{SR}(\lambda) - i_{90}^{SR}(\lambda)}{i_0^{SR}(\lambda) + i_{90}^{SR}(\lambda)} \tag{4.6}$$

With equations 4.4 and 4.6 the functions $F_0(\lambda)$ and $F_{90}(\lambda)$ in equations 4.1 and 4.2 are given by

$$F_{0/90}(\lambda) = \frac{1 \pm P^{SR}(\lambda)\ M(\lambda)}{1 \pm P^{TS}(\lambda)\ M(\lambda)} \tag{4.7}$$

To optimize the instrumentation for the calibration of the transfer source standards in a specific wavelength range, particular combinations of imaging mirror, grating and detector system have been used. Calibrations have been performed with two gratings, differing in line spacing and blaze angle, with two differently-coated, spherical mirrors and with two different photomultiplier detectors. For the source comparison the high-order performance of the gratings has been determined and its influence on the synchrotron radiation spectrum has been considered. Additionally, above 105 nm, LiF-filters have been used to suppress high-order contributions in the dispersed synchrotron radiation spectrum. For details on the NIM beam line see *Hollandt et al.* [1992] and *Hollandt et al.* [1994].

Due to the spectral range of the grazing-incidence source standard, it has been characterized from 15 nm to 60 nm with the TGM beam line and from 40 nm to 80 nm with the NIM beam line. From these measurements, twenty-five aluminium and rare-gas emission

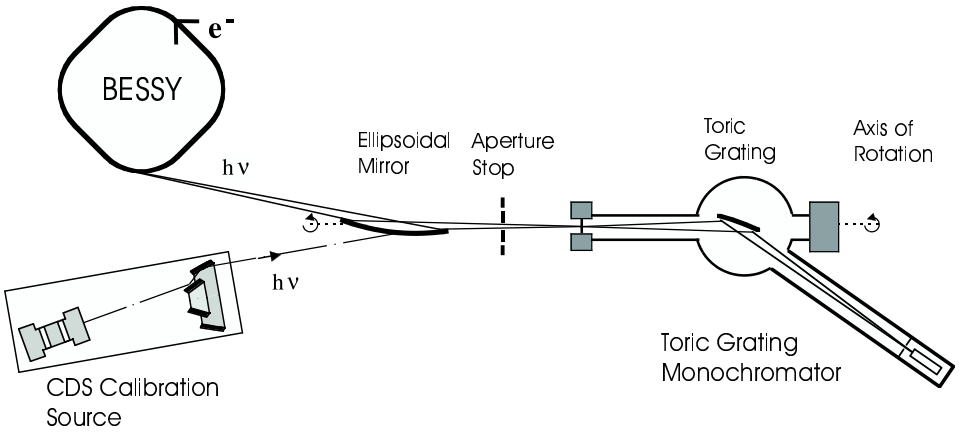

Figure 4.6: Schematic drawing of the grazing-incidence monochromator beam line for the radiometric calibration of transfer source standards in the 15 nm to 60 nm spectral range.

lines have been chosen for calibration. All these emission lines have been successively calibrated with adequate combinations of the optical elements, filters and detectors. Whenever possible the emission lines have been calibrated with at least two different configurations of the instrumentation to check for systematic uncertainties caused by inhomogeneity of the efficiency of the grating and high-order contributions in the dispersed synchrotron radiation spectrum.

The normal-incidence source standard could be characterized completely between 50 nm and 150 nm by use of the NIM beam line. In this spectral range, 32 rare-gas emission lines have been selected for calibration. Again, all emission lines have been calibrated with at least two different configurations of imaging mirror, grating and detector to check for systematic uncertainties. Additionally, a coarse cross-calibration with the VUV spectral responsivity scale, which is traceable to NIST, has been performed. For this purpose a NIST-calibrated Al_2O_3 photoemission diode has been brought into the collimated radiation of the normal-incidence source standard when the source has been operated with helium. The measured signal of the diode agreed well, within the combined uncertainty of the comparison (15 % at 1 σ level), with the calibrated photon flux of the source.

4.4 Results and Uncertainties

4.4.1 Photon Flux

The photon flux in the 25 selected emission lines of the grazing-incidence source standard is shown in Table 4.2. It ranges from 5×10^4 s^{-1} for the Al IV emission-line doublet (16.01 nm to 16.17 nm) to 2×10^8 s^{-1} for the He I resonance line at 58.43 nm. While the emitted radiation of the hollow-cathode source itself is unpolarized, the collimated radiation of the grazing-incidence source standard is partly polarized owing to the two grazing-incidence reflections in the Wolter telescope. Below 50 nm the polarization of the collimated radiation is less than 20 %. In the spectral range from 50 nm to 80 nm the polar-

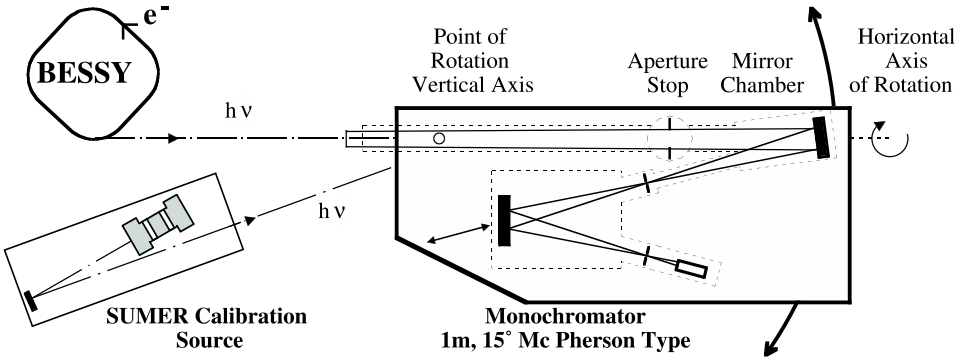

Figure 4.7: Schematic drawing of the normal-incidence monochromator beam line for the radiometric calibration of the transfer source standards in the 40 nm to 150 nm spectral range.

ization goes up to 50 %. Especially when calibrating an instrument with grazing-incidence optics at longer wavelengths, the significant polarization of the grazing-incidence source standard must be considered. Ideally, either the instrument or the source should be rotated by 90° around the axis of the collimated beam to correct for the polarization of the instrument.

The photon flux in the 32 selected emission lines of the normal-incidence source standard is shown in Table 4.3. It ranges from 4×10^6 s^{-1} for the Ar II emission line at 58.34 nm to 7×10^8 s^{-1} for the He I line at 58.43 nm. After only one reflection with an angle of incidence between the mirror normal and the incoming radiation of 3° the degree of polarization of the collimated radiation is less than 1 % for all emission lines.

4.4.2 Uncertainties

The overall uncertainty of the photon flux in the calibrated emission lines of Tables 4.2 and 4.3 originates from the uncertainty of the spectral photon flux of the primary standard BESSY, the uncertainties inherent in the comparison procedure of the transfer source standards with the primary standard and the long-term stability of the radiation emission of the transfer standards.

The spectral photon flux of the synchrotron radiation through the flux-limiting aperture stop of a source calibration beam line $\Phi_\lambda^{SR}(\lambda)$ is calculated according to Schwinger's formula. $\Phi_\lambda^{SR}(\lambda)$ is a function of six parameters $\Phi_\lambda^{SR}(\lambda) = \Phi_\lambda^{SR}(\lambda, W, B, I, a, d, \Psi_0)$. W is the energy of the stored electrons in the ring, B the magnetic induction in the bending magnet at the point of observation, and I is the current represented by the stored electrons.

PTB measured the standard electron energy of 800 MeV at BESSY I by means of resonant spin depolarization of the electrons [*Derbenev et al.*, 1980]. Since the characteristic polarization time of the electrons is proportional to W^{-5}, this method is not feasible for energies below 700 MeV, when the polarization time becomes longer than the life-time of the electrons stored in the ring. The flux comparison with the TGM beam line has been performed with the low electron-energy operation of BESSY of 340 MeV to reduce the synchrotron radiation diffracted in higher order in the spectrum. In the low-energy mode

Table 4.2: Radiant power and photon flux of selected emission lines of the grazing-incidence source standard – working point: 2 A, 400 V.

Wavelength / nm	Spectrum/buffer gas	Radiant Power / pW	Photon Flux / s^{-1}	Rel. standard uncertainty (1σ)
16.01/16.17	Al IV / Ne	0.67	$5.43\ 10^4$	8 %
16.95-17.56	Al III / Ne	1.41	$1.22\ 10^5$	8 %
16.01/16.17	Al IV / Ar	0.60	$4.86\ 10^4$	8 %
16.95-17.56	Al III / Ar	1.01	$8.77\ 10^4$	8 %
20.43-20.89	Ne IV	3.3	$3.43\ 10^5$	8 %
21.26	Ne IV	1.15	$1.23\ 10^5$	8 %
21.54-21.88	Ne IV	4.4	$4.81\ 10^5$	8 %
22.26-22.36	Ne IV	1.81	$2.03\ 10^5$	8 %
26.71-26.77	Ne III	7.5	$1.01\ 10^6$	8 %
28.25-28.39	Ne III	18.3	$2.61\ 10^6$	7 %
30.11	Ne III	10.2	$1.55\ 10^6$	7 %
30.38	He II	320	$4.89\ 10^7$	7 %
30.86	Ne III	4.0	$6.21\ 10^5$	7 %
31.31-31.39	Ne III	12.4	$1.96\ 10^6$	7 %
37.93	Ne III	57	$1.09\ 10^7$	7 %
40.59/40.71	Ne II	98	$2.01\ 10^7$	7 %
44.50-44.78	Ne III	173	$3.89\ 10^7$	7 %
46.07-46.24	Ne II	676	$1.57\ 10^8$	7 %
48.81-49.11	Ne III	71	$1.75\ 10^7$	7 %
53.70	He I	26.5	$7.16\ 10^6$	7 %
58.43	He I	609	$1.79\ 10^8$	7 %
71.81-74.53	Ar II	69	$2.54\ 10^7$	7 %
73.59	Ne I	271	$1.00\ 10^8$	7 %
74.37	Ne I	157	$5.88\ 10^7$	7 %
76.92	Ar III	5.8	$2.25\ 10^6$	7 %

Table 4.3: Radiant power and photon flux of selected emission lines of the normal-incidence source standard – working point: 1 A, 500 V.

Wavelength / nm	Spectrum	Radiant Power / pW	Photon Flux / s^{-1}	Rel. standard uncertainty (1σ)
53.70	He I	55.3	$1.49\ 10^{7}$	6 %
54.29 / 54.32	Ar II	50.9	$1.39\ 10^{7}$	6 %
54.75	Ar II	67.9	$1.87\ 10^{7}$	6 %
58.34	Ar II	14.3	$4.20\ 10^{6}$	6 %
58.43	He I	2394	$7.04\ 10^{8}$	6 %
60.29 / 60.42	Ar II / Ar III	19.8	$6.02\ 10^{6}$	6 %
61.24	Ar II	13.6	$4.19\ 10^{6}$	6 %
67.09 - 67.29	Ar II	66.9	$2.26\ 10^{7}$	6 %
71.81	Ar II	18.8	$6.80\ 10^{6}$	7 %
72.20	Kr III	33.5	$1.22\ 10^{7}$	7 %
72.34 / 72.55	Ar II	68.1	$2.48\ 10^{7}$	7 %
73.09	Ar II	23.0	$8.47\ 10^{6}$	7 %
73.59	Ne I	955	$3.54\ 10^{8}$	7 %
74.03	Ar II	55.7	$2.08\ 10^{7}$	7 %
74.37	Ne I	526	$1.97\ 10^{8}$	7 %
74.49 / 74.53	Ar II	42.5	$1.59\ 10^{7}$	7 %
76.92	Ar III	24.7	$9.56\ 10^{6}$	7 %
88.41 / 88.63	Kr II	212	$9.45\ 10^{7}$	7 %
89.10	Kr II	75.8	$3.40\ 10^{7}$	7 %
91.74	Kr II	382	$1.77\ 10^{8}$	7 %
91.98	Ar II	812	$3.76\ 10^{8}$	7 %
93.21	Ar II	486	$2.28\ 10^{8}$	7 %
96.50	Kr II	455	$2.21\ 10^{8}$	7 %
104.82	Ar I	508	$2.68\ 10^{8}$	7 %
106.67	Ar I	406	$2.18\ 10^{8}$	7 %
110.04	Xe II	108	$5.98\ 10^{7}$	7 %
115.85	Xe II	47.6	$2.78\ 10^{7}$	7 %
116.49	Kr I	136	$7.98\ 10^{7}$	6 %
118.31	Xe II	95.0	$5.66\ 10^{7}$	6 %
123.58	Kr I	421	$2.62\ 10^{8}$	6 %
124.48	Xe II	22.5	$1.41\ 10^{7}$	6 %
146.96	Xe I	200	$1.48\ 10^{8}$	6 %

of BESSY the electron energy has been determined from an absolute measurement of the synchrotron radiation spectrum measured with a calibrated, energy-dispersive, Si(Li) detector [*Tegeler and Ulm*, 1988].

The magnetic induction was measured by a nuclear magnetic resonance probe in the center of the dipole magnet. Since the tangent points of both source calibration beam lines are not in the center of the dipole magnet, the uncertainty of B is dominated by the field inhomogeneity along the electron path, which has been measured relatively with a Hall probe.

To measure the electron current over the full range from 0.8 pA (one stored electron in the ring) up to 1 A, PTB is using three different methods [*Ulm et al.*, 1989]. While small currents up to 1000 stored electrons are accurately measured by single-electron counting [*Riehle et al.*, 1988], a current above 0.5 mA is measured, with an uncertainty of 5 μA, by two identical dc-beam-current transformers. For the calibration of the transfer source standards the storage ring has been operated with an electron current of typically 100 μA to adjust the accepted photon flux of the synchrotron radiation to the photon flux of the transfer standards. In this intermediate current range (0.8 nA $<$ I $<$ 1.5 mA) the current is measured by means of different photodiodes, which have to be calibrated against the current transformer at typically 1 mA. The uncertainty of the current measurement is therefore dominated by the calibration uncertainty and the linearity of the photodiodes.

The angle Ψ_0 of the center of the flux-limiting aperture with respect to the electron orbit plane was determined from the measured vertical angular distribution of the synchrotron radiation. Additionally, the size of the aperture stop a and its distance d from the tangent point of observation had to be measured. A description of the measurement procedure is given in *Thornagel et al.* [1996].

In Table 4.4 the influence of the uncertainties of the storage ring parameters and the geometrical quantities on the uncertainty of the spectral photon flux of BESSY I is shown for typical wavelengths of the two source-calibration beam lines. For all measurements with the two source standards, the relative standard uncertainty of the spectral photon flux of the synchrotron radiation has been below 2.5 %. It should be mentioned that, for precision experiments, a significantly smaller uncertainty of the spectral photon flux of the synchrotron radiation was achieved at BESSY I [*Arnold and Ulm*, 1992; *Thornagel et al.*, 1996].

In the overall uncertainty of the photon flux of the transfer standards, the main contributions of the comparison procedure stem from spatial variations of the grating efficiency and the detector responsivity. Therefore, it has been of crucial importance for the flux comparison to illuminate, as far as possible, identical areas on the grating and on the detector by both the transfer and primary standards. The uncertainties resulting from the inhomogeneities of the optical components and the detectors were determined from measurements of the synchrotron radiation with aperture stops of different sizes, which resulted in slightly different responsivities of the instrumentation used in the flux comparison.

Additionally, in general, the synchrotron radiation signal $i^{SR}(\lambda)$ contains radiation diffracted in higher order. With the TGM beam line, the contribution of high-order diffraction to the uncertainty of the flux comparison is reduced to 1 % by the use of filters and a reduced electron energy (340 MeV). With the NIM beam-line no filters have been applied below 105 nm and the influence of second-order diffracted radiation could be corrected from the knowledge of the high-order performance of the gratings employed. The uncertainty of this correction strongly depends on the observed wavelength and the imaging

Table 4.4: Contributions to the relative uncertainty (1σ) of the spectral photon flux of the synchrotron radiation.

Source of uncertainty	Value for TGM beam line	Rel. std. uncertainty $\Delta\Phi\lambda^{SR}/\Phi\lambda^{SR}$ at 40 nm	Value for NIM beam line	Rel. std. uncertainty $\Delta\Phi\lambda^{SR}/\Phi\lambda^{SR}$ at 90 nm
Electron energy	W = (337 $\pm$2) MeV	0.99 %	W = (798 $\pm$ 1) MeV	0.09 %
Magnetic induction	B = (0.631$\pm$0.005) T	0.13 %	B = (1.482$\pm$ 0.005) T	0.23 %
Electron current: Diode calibration at Linearity of diode	I = (1500$\pm$ 5) μA $\pm$ 0.5 %	0.60 %	I = (1500 $\pm$5) μA $\pm$ 0.5 %	0.60 %
Diameter of aperture stop	a = (5.286 $\pm$ 0.010) mm	0.38 %	a = (10.00 $\pm$ 0.02) mm	0.40 %
Distance of aperture stop	d = (15050 $\pm$ 15) mm	0.20 %	d = (23745 $\pm$ 50) mm	0.42 %
Emission angle	Ψ_0 = (0.04 $\pm$ 0.02) mrad	0.01 %	Ψ_0 = (0.50 $\pm$ 0.05) mrad	0.93 %
Beam emittance: vertical beam divergence vertical beam size	 $\pm$ 30 μrad $\pm$ 500 μm	 } 0.03 %	 $\pm$ 30 μrad $\pm$ 500 μm	 } 0.01 %
Total sum in quadrature $\Delta\Phi\lambda^{SR}/\Phi\lambda^{SR}$		**1.2 %**		**1.3 %**

mirror used. As mentioned earlier, LiF filters were used to suppress radiation diffracted in higher order above 105 nm.

In Table 4.5 the contributions of the primary standard BESSY I, of the comparison procedure and of the stability of the hollow-cathode source to the uncertainty of the photon flux of the transfer standards are given for two different wavelengths and two different optical configurations of the NIM beam-line. The overall relative uncertainty of the photon flux in the calibrated emission lines results from the sum, in quadrature, of these contributions and is listed in Table 4.2 and Table 4.3.

4.5 Summary

We describe transfer source standards based on hollow-cathode, glow discharges which can be used for the overall radiometric calibration of VUV astronomical instrumentation. Our standards have a photon flux that is traceable to the electron storage ring BESSY I, a primary radiometric standard, and produce a collimated beam that can directly irradiate the telescope entrance aperture. The source standards are transportable, and their differential pumping system permits windowless operation in connection with an ultrahigh-vacuum system.

Calibration can thus take place in the tank that is used for instrument development and testing; the instrument need not be transported to a special calibration facility. Scheduling problems, as they are bound to occur with the primary synchrotron source standards, are

Table 4.5: Overall relative uncertainty (1σ) of the photon flux of the normal-incidence source standard.

Source of uncertainty	at 55 nm		at 90 nm	
	Imaging mirror:			
	Au	SiC	Au	SiC
Spectral photon flux of synchrotron radiation	1.4 %	1.4 %	1.3 %	1.3 %
Synchrotron radiation diffracted in high-order	–	–	2.5 %	0.6 %
Inhomogeneity of optical components and detector	3.0 %	3.5 %	3.0 %	3.5 %
Linearity of detector	0.6 %	0.6 %	0.6 %	0.6 %
Wavelength calibration	0.4 %	0.9 %	0.1 %	0.1 %
Stability of hollow cathode source	5 %	5 %	5 %	5 %
Total sum in quadrature $\Delta\Phi\lambda^{SR}/\Phi\lambda^{SR}$	**6.0 %**	**6.4 %**	**6.5 %**	**6.3 %**

also avoided. The transfer source standards produce a line spectrum so that they can be used for both radiometric and wavelength calibration; order-sorting is straightforward.

The diameters of the collimated beams (5 mm and 10 mm) are small compared to those of a typical (solar or non-solar) space-telescope entrance-aperture (100 mm to several meters). This permits a mapping of local spectral-responsivity variations over the telescope aperture. At the same time, the small, collimated, input beams generate instrument count-rates typical of those expected in flight, since their photon flux corresponds to that typically collected in flight by the entire telescope aperture.

Accordingly, these transportable source standards are suitable for the calibration not only of solar VUV instruments (for which they were originally developed), but also for astronomical space instrumentation in general. Two of the instruments flown on SOHO, CDS (Coronal Diagnostic Spectrometer, *Harrison et al.* [1995]) and SUMER (Solar Ultraviolet Measurements of Emitted Radiation, *Wilhelm et al.* [1995]), have been calibrated by use of the systems described in this paper [*Hollandt et al.*, 1996; *Lang et al.*, 2000].

The photon flux of the source standards is known to better than 8 % (1σ value). This is clearly adequate for the current requirement for quantitative solar spectroscopy, particularly in the extreme-ultraviolet spectral domain, where accuracy is limited by the larger uncertainties in the atomic data used in diagnostic investigations of solar plasma [*Mason and Monsignori-Fossi*, 1994].

We maintain that the existence of a reliable laboratory standard is a prerequisite for verifying the radiometric stability of an instrument, as long as it is on the ground. Particularly, collimated source standards, such as those described here, provide a precise means of testing the radiometric stability of the entire, assembled system, rather than only of its individual optical components.

As indicated in the introduction, at the radiometry laboratory of PTB at BESSY, an improved primary detector standard – an electrical substitution radiometer operating at

liquid-helium temperature [*Rabus et al.*, 1997] – has achieved significantly lower uncertainties. In the spectral range between 40 nm and 400 nm, the spectral responsivity of photodiodes has been determined with a relative uncertainty better than 1 %, the results being in good agreement with a calibration against the laser-operated cryogenic radiometer of PTB Berlin [*Rabus et al.*, 1997]. Similar progress has also been made in the determination of the spectral responsivity of photodiodes with this method in the soft X-ray range (0.1 nm to 25 nm) [*Krumrey et al.*, 2000]. Such well-characterized transfer detector standards, in combination with collimated monochromatized radiation, offer the potential to calibrate complete astronomical telescopes at special synchrotron radiation beam lines with smaller uncertainties than those realized in the past. A beam line of this kind is planned at the radiometry laboratory of PTB at the electron storage ring BESSY II.

Acknowledgements

We thank E. Tegeler and G. Ulm for many helpful discussions. We also thank M. Bock, P. Klein, and W. Paustian for their valuable technical support. This work was financially supported by the European Space Agency (Contract No.9419/91/F/BZ) and the Max-Planck-Institut für Aeronomie.

Bibliography

Arnold, D., and Ulm, G., Electron storage ring BESSY as a source of calculable spectral photon flux in the X-ray region, *Rev. Sci. Instrum.* **63**, 1539, 1992.

Besson, J.C., Certain, P., Dael, A. et al., Super-ACO: Results on a positron low emittance ring, *Rev. Sci. Instrum.* **60**, 1373, 1989.

Canfield, L.R., and Swanson, N., Far ultraviolet detector standards, *Journal of Research of the National Bureau of Standards* **92**, 97, 1987.

Danzmann, K., Günther, M., Fischer, J., Kock, M., and Kühne, M., High current hollow cathode as a radiometric transfer standard source for the extreme vacuum ultraviolet, *Appl. Opt.* **27**, 4947, 1988.

Derbenev, Y.S., Kondratenko, A.M., Serednyakov, S.I., Skrinsky, A.N., Tumaikin, G.M.,and Shatunov, Y.M., Accurate calibration of the beam energy in a storage ring based on measurement of spin precession frequency of polarized particles, *Particle Accel.* **10**, 177, 1980.

Fischer, J., Kühne, M., and Wende, B., Instrumentation for spectral radiant power measurements of sources in the wavelength range from 5 to 150 nm using the electron storage ring BESSY as a radiometric standard source, *Nucl. Instrum. Methods A* **246**, 404, 1986.

Furst, M.L., Graves, R.M., Canfield, L.R., and Vest, R.E., Radiometry at the NIST SURF II storage ring facility, *Rev. Sci. Instrum.* **66**, 2257, 1995.

Harrison, R.A., Sawyer, E.C., Carter, M.K., Cruise, A.M., Cutler, R.M., Fludra, A., Haynes, R.W., Kent, B.J., Lang, J., Parker, D.J., Payne, J., Pike, C.D., Peskett, S.C., Richards, A.G., Culhane, J.L., Norman, K., Breeveld, A.A. Breeveld, E.R., Al Janabi, K.F., McCalden, A.J., Parkinson, J.H., Self, D.G., Thomas, P.D., Poland, A.I., Thomas, R.J., Thompson, W.T., Kjeldseth-Moe, O., Brekke, P., Karud, J., Maltby, P., Aschenbach, B., Bräuninger, H., Kühne, M., Hollandt, J., Siegmund, O.H.W., Huber, M.C.E.,

Gabriel, A.H., Mason, H.E., and Bromage, B.J.I., The Coronal Diagnostic Spectrometer for the Solar and Heliospheric Observatory, *Sol. Phys.* **162**, 233, 1995.

Henke, B.L., and Tester, M.A., Techniques of low energy X-ray spectroscopy, *Adv. X-Ray Anal.* **18**, 76, 1975.

Hollandt, J., Jans, W., Kühne, M., Lindenlauf, F., and Wende, B., A beam line for radiant power measurements of vacuum ultraviolet and ultraviolet sources in the wavelength range 40 – 400 nm, *Rev. Sci. Instrum.* **63**, 1278, 1992.

Hollandt, J., Huber, M.C.E., and Kühne, M., Hollow cathode transfer standards for the radiometric calibration of VUV telescopes of the Solar and Heliospheric Observatory, *Metrologia* **30**, 381, 1993.

Hollandt, J., Kühne, M., and Wende, B., High-current hollow-cathode source as a radiant intensity standard in the 40 – 125 nm wavelength range, *Appl. Opt.* **33**, 68, 1994.

Hollandt, J., Schühle, U., Paustian, W., Curdt, W., Kühne, M., Wende, B., and Wilhelm, K., Radiometric calibration of the telescope and ultraviolet spectrometer SUMER on SOHO, *Appl. Opt.* **35**, 5125, 1996.

Kroth, U., Saito, T., and Tegeler, E., Quantum efficiency of a semiconductor photodiode in the VUV determined by comparison with a proportional counter in monochromatized synchrotron radiation, *Appl. Opt.* **29**, 18, 1990.

Krumrey, M., Herrmann, C., Müller, P., and Ulm, G., Synchrotron-radiation-based cryogenic radiometry in the X-ray range, *Metrologia* **37**, 361, 2000.

Kühne, M., and Müller, P., Higher order contributions in the synchrotron radiation spectrum of a toroidal grating monochromator determined by the use of a transmission grating, *Rev. Sci. Instrum.* **60**, 2101, 1989.

Lang, J., Kent, B.J., Breeveld, A.A., Breeveld, E.R:, Bromage, B.J.I., Hollandt, J., Payne, J., Pike, C.D., and Thompson, W.T., The laboratory calibration of the SOHO Coronal Diagnostic Spectrometer, *J. Opt. A* **2**, 88, 2000.

Lemaire, P., Sensitivity changes in the CNRS ultraviolet spectrometer aboard OSO-8, *ESA J.* **15**, 237, 1991.

Mason, H.E., and Monsignori Fossi, B., Spectroscopic diagnostics in the VUV for solar and stellar plasmas, *Astron. Astrophys. Rev.* **6**, 123, 1994.

Philips, R., Sources and applications of ultraviolet radiation, Academic Press, London, p. 138 and citations therein, 1984.

Rabus, H., Scholze, F., Thornagel, R., and Ulm, G., Detector calibration at the PTB radiometry laboratory at BESSY, *Nucl. Instrum. Methods A* **377**, 209, 1996.

Rabus, H., Persch, V., and Ulm, G., Synchrotron-radiation-operated cryogenic electrical substitution radiometer as the high-accuracy primary detector standard in the ultraviolet, vacuum-ultraviolet, and soft-X-ray spectral ranges, *Appl. Opt.* **36**, 5421, 1997.

Reeves, E.M., Timothy, J.G., Huber, M.C.E., and Withbroe, G.L., Photometric calibration of the EUV spectroheliometer on ATM, *Appl. Opt.* **16**, 849, 1977.

Riehle, F., Bernstorff, S., Fröhling, R., and Wolf, F.P., Determination of electron currents below 1 nA in the storage ring BESSY by measurement of the synchrotron radiation of single electrons, *Nucl. Instrum. Methods A* **268**, 262, 1988.

Samson, J.A.R., Absolute intensity measurement in the vacuum ultraviolet, *J. Opt. Soc. Am.* **54**, 6, 1964.

Samson, J.A.R., and Haddad, G.N., Absolute photon flux measurement in the vacuum ultraviolet, *J. Opt. Soc. Am.* **64**, 47, 1974.

Schwinger, J., On the classical radiation of accelerated electrons, *Phys. Rev.* **75**, 1912,

1949.

Shaw, P.-S., Lykke, K.R., Gupta, R., O'Brien, T.R., Arp, U., White, H.H., Lucartorto, T.B., Dehmer, J.L., and Parr, A.C., Ultraviolet radiometry with synchrotron radiation and cryogenic radiometry, *Appl. Opt.* **38**, 18, 1999.

Tegeler, E., and Ulm, G., Determination of the beam energy of an electron storage ring by using calibrated energy dispersive Si(Li)-detectors, *Nucl. Instr. and Meth. A* **266**, 185, 1988.

Thornagel, R., Fischer, J., Friedrich, R., Stock, M., Ulm, G., and Wende, B., The electron storage ring BESSY as a primary standard source – a radiometric comparison with a cryogenic electrical substitution radiometer in the visible, *Metrologia* **32**, 459, 1996.

Ulm, G., Hänsel-Ziegler, W., Bernstorff, S., and Wolf, F.P., Measuring devices at BESSY for stored beam currents ranging from 0.8 pA to 1 A, *Rev. Sci. Instrum.* **60**, 1752, 1989.

Wilhelm, K., Curdt, W., Marsch, E., Schühle, U., Lemaire, P., Gabriel, A., Vial, J.-C., Grewing, M., Huber, M.C.E., Jordan, S.D., Poland, A.I., Thomas, R.J., Kühne, M., Timothy, J.G., Hassler, D.M., and Siegmund, O.H.W., SUMER-Solar Ultraviolet Measurements of Emitted Radiation, *Sol. Phys.* **162**, 189, 1995.